

Supporting Information for:

**Electron Energy Loss of Terrylene Deposited on Au(111):
Vibrational and Electronic Spectroscopy**

P. Navarro¹, F.C. Bocquet^{2,3}, I. Deperasińska⁴, G. Pirug^{2,3}, F. S. Tautz^{2,3}, M. Orrit¹

¹ *Huygens-Kamerlingh Onnes Laboratory, University of Leiden
2300 RA Leiden (Netherlands)*

² *Peter Grünberg Institut (PGI-3), Forschungszentrum Jülich, 52425 Jülich (Germany)*

³ *Jülich-Aachen Research Alliance (JARA), Fundamentals of Future Information Technology,
52425, Jülich (Germany)*

⁴ *Institute of Physics, Polish Academy of Sciences, 02-668, Warsaw (Poland)*

S1. Deposition of Terrylene on Au(111) followed by XPS

Figure S1 shows the evolution of the XPS intensity signals after exposure of the Au(111) surface to terrylene. The spectra show the expected doublet peak for gold, which corresponds to the Au $4f_{7/2}$ electrons with binding energy of 87.1 eV and the Au $4f_{5/2}$ electrons with binding energy of 87.8 eV. The signal decreases as terrylene is deposited on the gold surface.

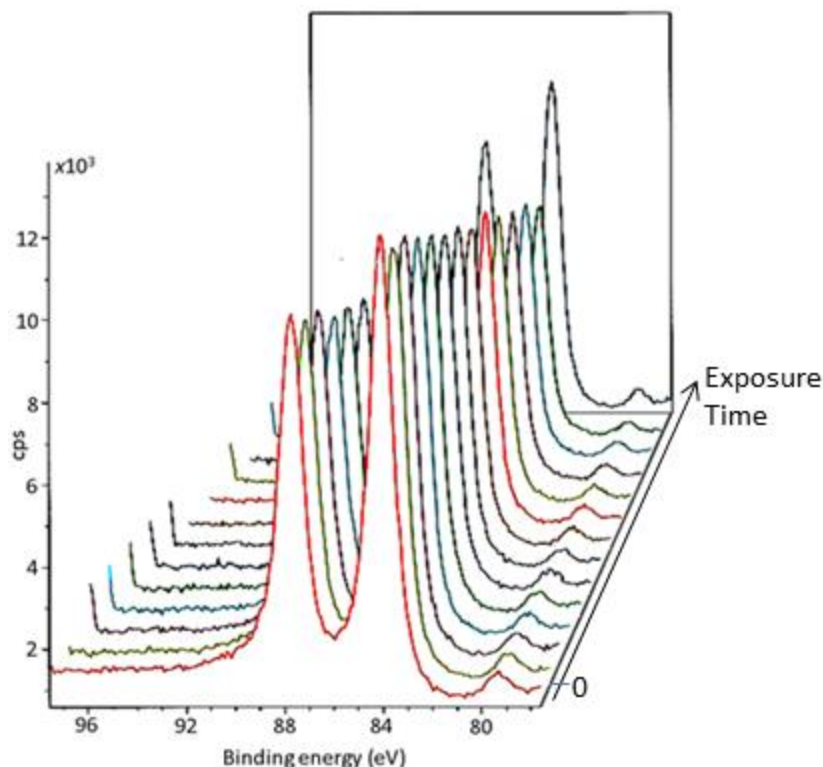


Figure S1a : The first XPS spectrum corresponds to the clean Au(111) surface before deposition of terrylene. The peak at 87.8 eV corresponds to the Au $4f_{7/2}$ and the peak at 84.1 eV to the Au $4f_{5/2}$. The deposition times for each spectrum were 2, 4, 6, 8, 10, 12, 14, 16, 18, 20, 22, 27 and 42 min exposure. The last spectrum corresponds to clean surface again after sputtering. The temperature in the Knudsen cell was $198 \pm 2^\circ\text{C}$.

Figure S1b shows the increasing XPS signal of the C1s electrons with binding energy 284.2 eV as a function of increasing exposure of the gold surface to terrylene and show the complementary growth of the carbon signal.

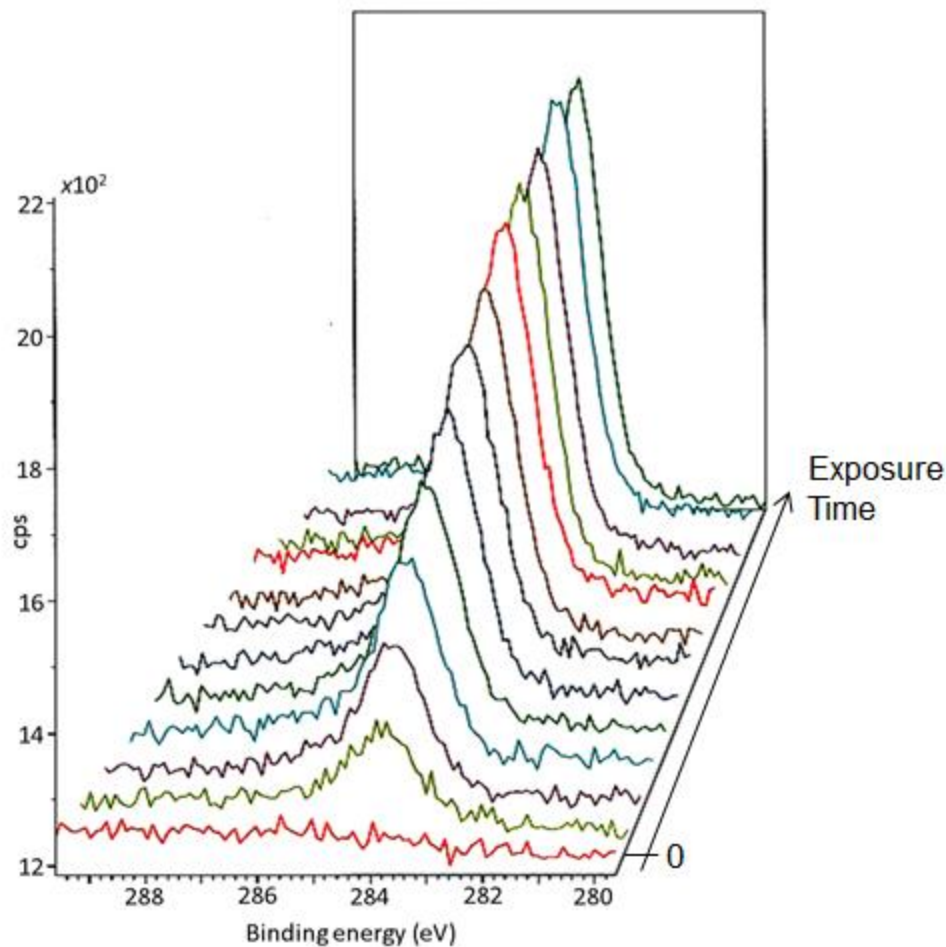


Figure S1b: XPS spectra of Au(111) at various deposition stages of terrylene films in the carbon region, for the C1s signal. Same conditions as for Fig. S1a.

Figure S1c shows the integrated intensity from the correspondent peaks in Figs. S1a and b, respectively. One can clearly observe the decrease of the *Au* signal correlated to the increase of *C* signal due to the deposition of terrylene in the surface. The HREEL spectra shown in Fig.3 (main text) and in Fig.S2, were taken exactly after recording these XPS spectra. In this way we followed the evolution of the HREEL spectra as a function of increasing terrylene deposition.

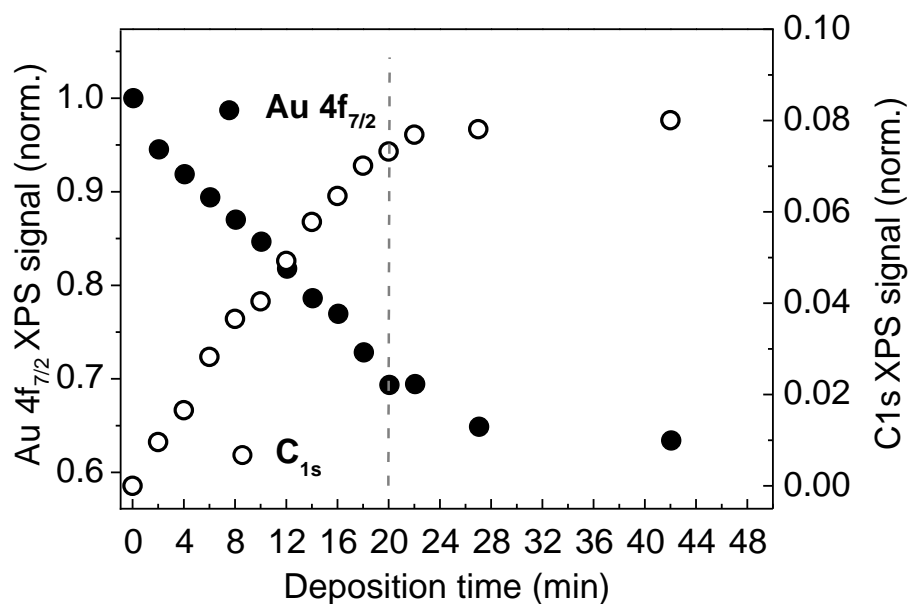


Figure S1 c: Filled dots (●) show the integrated intensity of the Au 4f_{7/2} electrons with binding energy 84.1 eV. Empty dots (○) show the C1s electrons with binding energy 284.2 eV. Both signals were normalized to the Au 4f_{7/2} intensity obtained for the clean gold surface before and after the experiment. The dotted line indicates when the surface presumably becomes fully covered with terrylene. The gold signal decays to about 60% of the maximum, showing that terrylene is not deposited as a uniform film any more. This points to a Stranski-Krastanov growth mode.

S2. HREEL at increasing deposition times

The data shown in Fig.S2 correspond to the HREEL spectra for increasing deposition of terrylene. These were taken after each exposition shown in Fig S1. Figure 3 shows data for very high exposition times where clear changes on the HREELS can be observed. Therefore, the data in Fig.S2 complements data on Fig. 3 (main text). The main peak at 802 cm^{-1} appears even after the shortest deposition time (2 min), where other features can barely be seen. The very weak intensity in the *in-plane* region 1280 and 1495 cm^{-1} (insert zoom $40\times$) can be due to the electrostatic image effect of the gold surface.

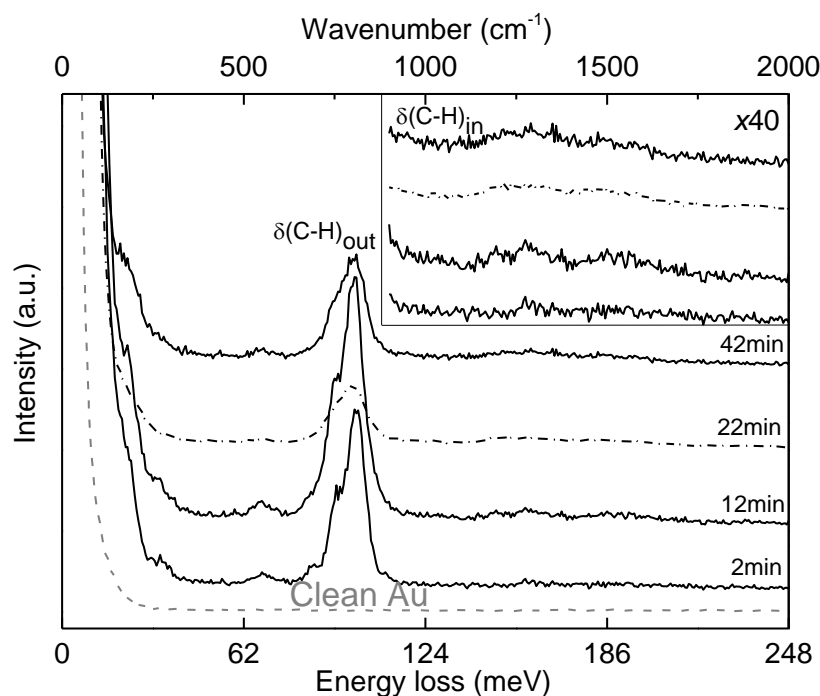


Figure S2: The specular HREELS spectra as a function of increasing deposition time of terrylene on a clean gold surface (dotted spectrum) up to 42 min. The beam energy used was $E_0 = 5\text{ eV}$ and the integration time was 30 min. The insert shows the same energy interval from $800 - 2000\text{ cm}^{-1}$, magnified by a factor of 40.

S3. Optical spectroscopy of terrylene in solution

This spectrum is useful to compare the electronic excitation of our terrylene films by electron impact in Fig.4 with the optical excitation of the HOMO \rightarrow LUMO transition of terrylene in solution. The maximum absorption peak appears at $17\,699\text{ cm}^{-1}$ with a 0-1 vibronic component at $19\,157\text{ cm}^{-1}$.

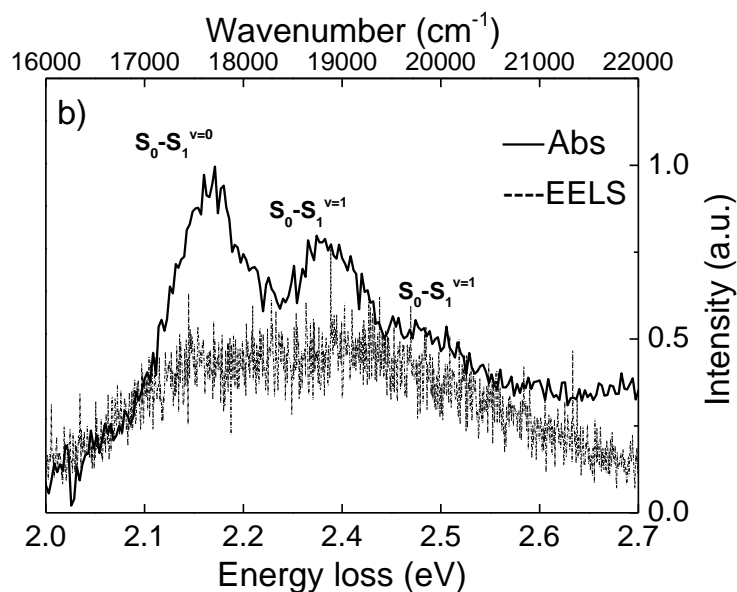
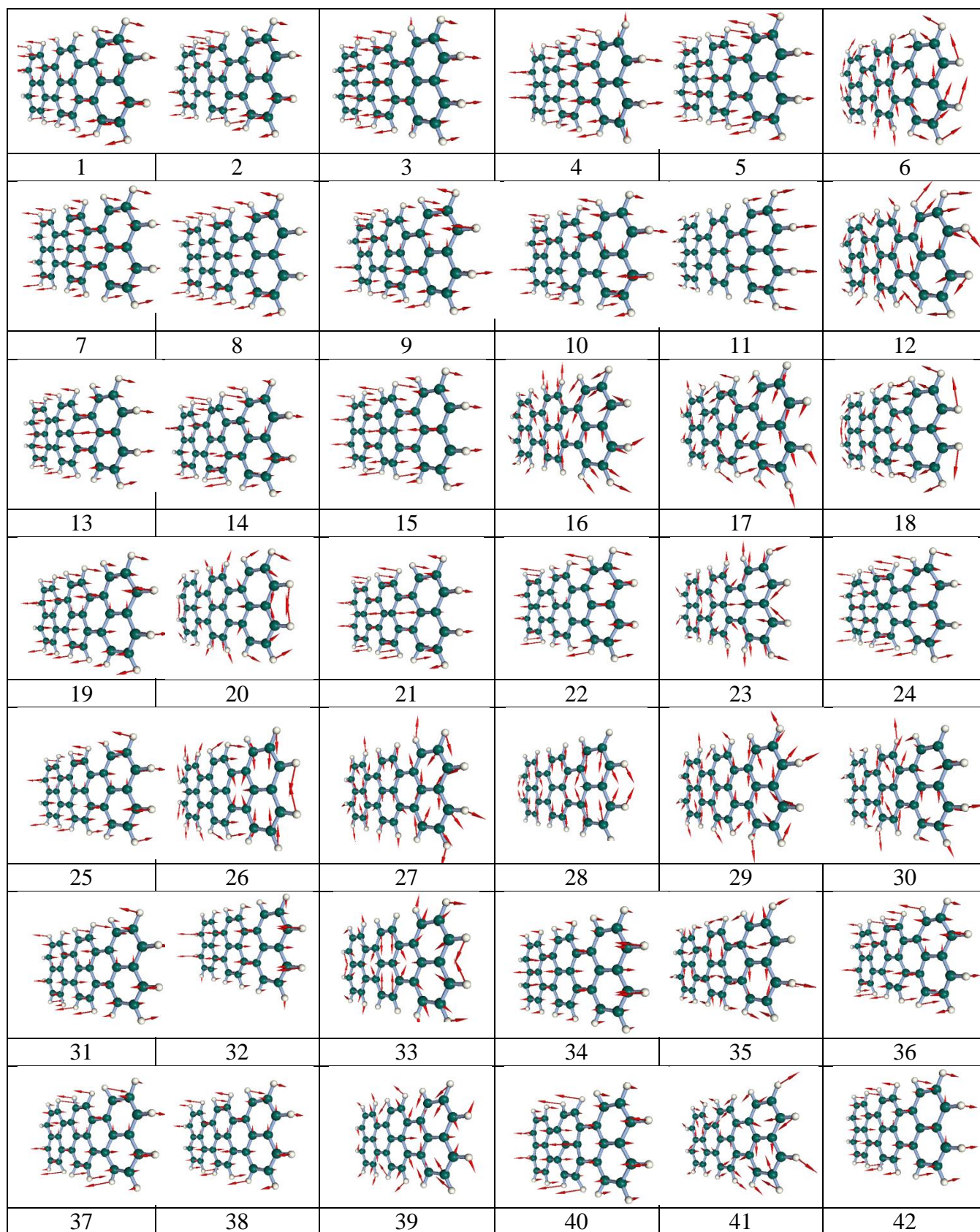


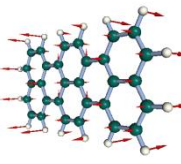
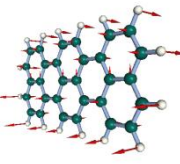
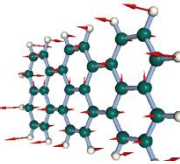
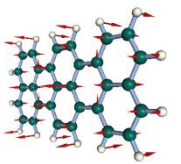
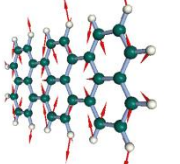
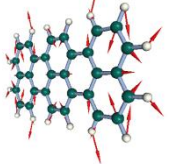
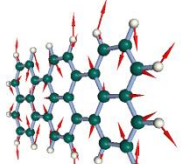
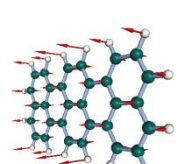
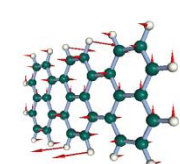
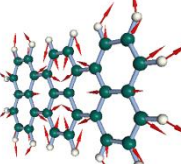
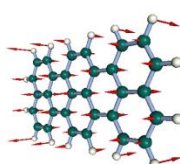
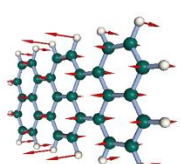
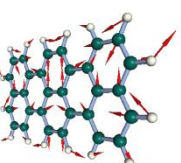
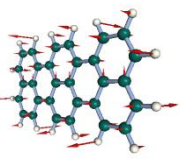
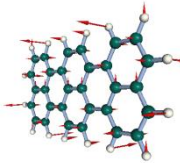
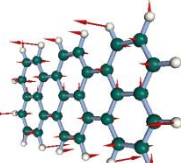
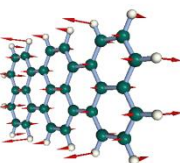
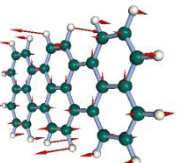
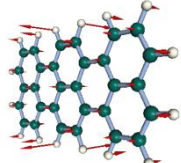
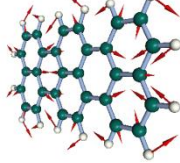
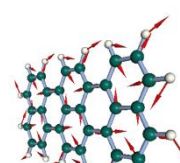
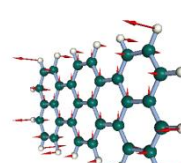
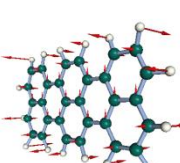
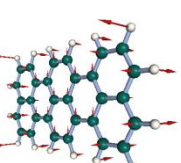
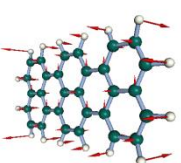
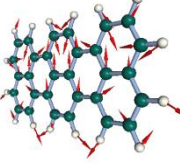
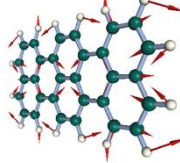
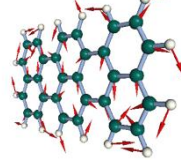
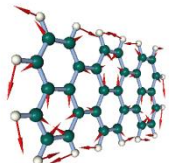
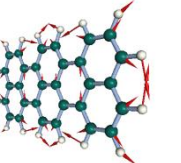
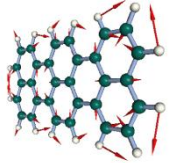
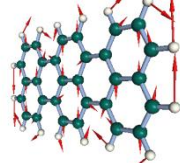
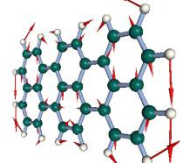
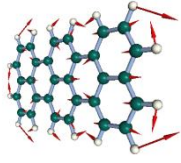
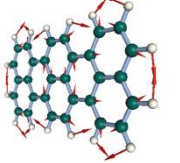
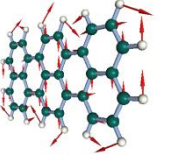
Figure S3: Solid line: absorption spectrum of a terrylene solution in ortho-dichlorobenzene. The dashed line is the HREELS spectrum of Fig.4 reproduced for comparison (the upper axis shows the wavenumber of the optical spectrum, compared to the energy loss on the lower axis).

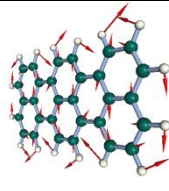
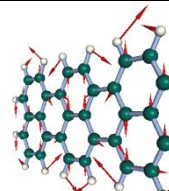
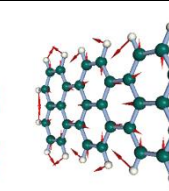
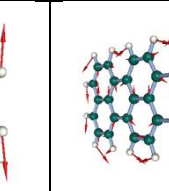
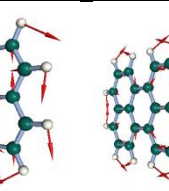
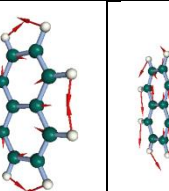
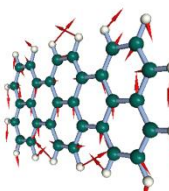
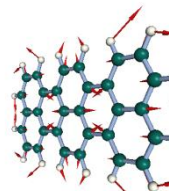
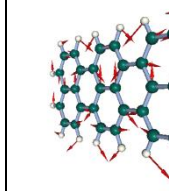
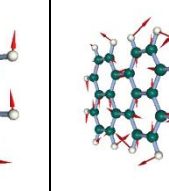
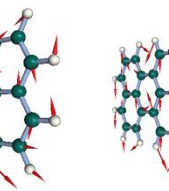
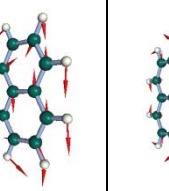
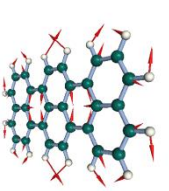
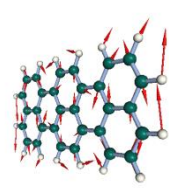
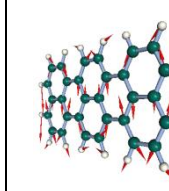
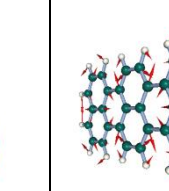
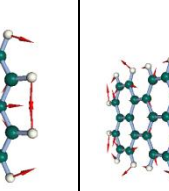
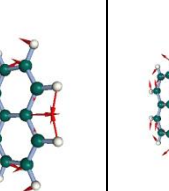
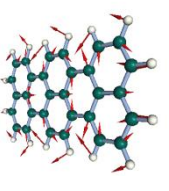
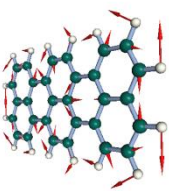
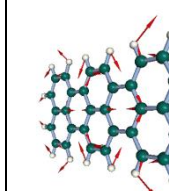
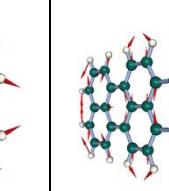
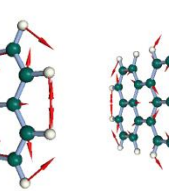
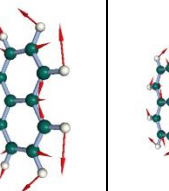
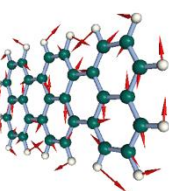
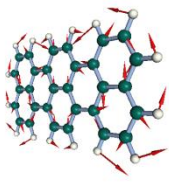
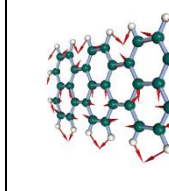
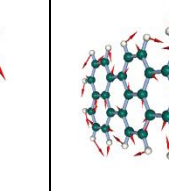
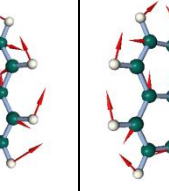
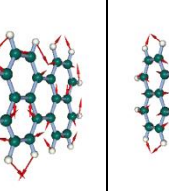
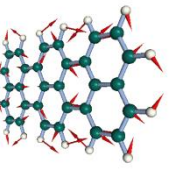
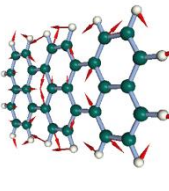
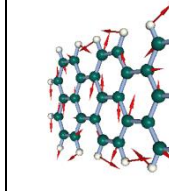
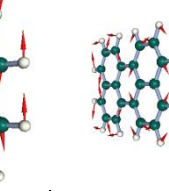
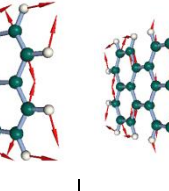
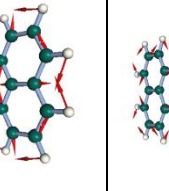
Table S1: Symmetry, frequencies, IR activity, and reduced masses of the 132 ground-state vibrations of terrylene calculated with the DFT B3LYP/6-31 G(d,p) method. Below: visualization of normal modes (visualization with the use of Facio 16.2.1)

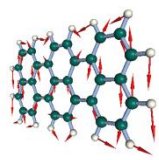
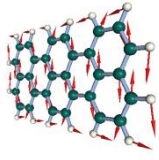
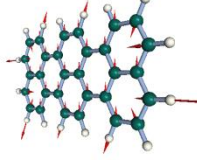
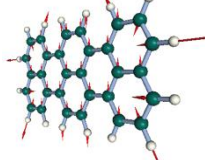
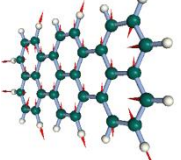
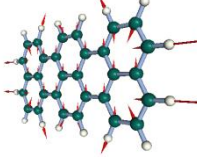
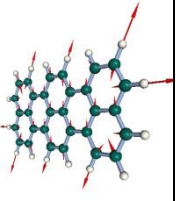
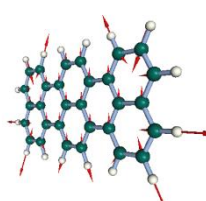
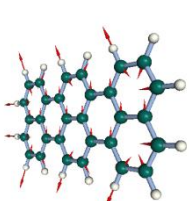
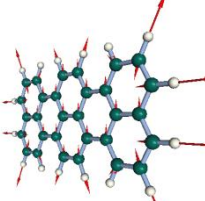
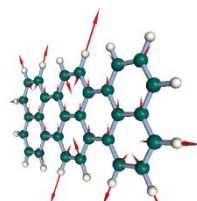
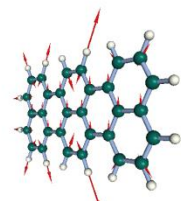
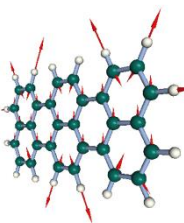
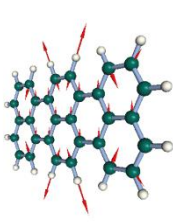
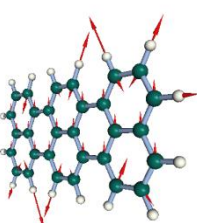
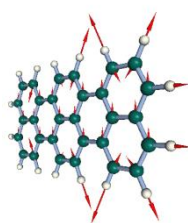
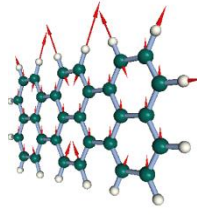
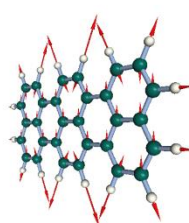
no	sym	(cm ⁻¹)	IR	red.mass	in plane / out of plane	no	sym	(cm ⁻¹)	IR	red.mass	in plane / out of plane
1	AU	20.7	0.0	4.937	out	67	B2G	980.0	0.0	1.304	out
2	B1G	28.4	0.0	4.400	out	68	B2U	1044.5	2.7285	7.010	in
3	B3U	36.9	0.1459	5.706	out	69	AG	1058.9	0.0	3.752	in
4	B2G	111.6	0.0	4.790	out	70	B3G	1081.0	0.0	3.950	in
5	B3U	112.3	0.1231	3.462	out	71	B2U	1093.2	2.6642	2.735	in
6	B2U	150.3	0.0906	5.705	in	72	AG	1125.5	0.0	1.782	in
7	B2G	168.3	0.0	4.301	out	73	B1U	1126.3	3.0817	1.900	in
8	B3U	181.1	4.6656	4.251	out	74	B3G	1160.8	0.0	1.611	in
9	AU	214.2	0.0	4.032	out	75	B2U	1173.1	2.5283	1.372	in
10	B1G	221.0	0.0	3.565	out	76	B1U	1186.0	0.0001	1.683	in
11	AG	246.4	0.0	7.576	in	77	AG	1186.0	0.0	1.294	in
12	B3G	276.9	0.0	5.695	in	78	B3G	1198.5	0.0	2.050	in
13	B3U	277.2	1.4772	5.750	out	79	B3G	1218.4	0.0	1.481	in
14	AU	297.9	0.0	3.916	out	80	B2U	1222.8	0.0613	1.558	in
15	B2G	353.3	0.0	4.574	out	81	B1U	1232.4	7.6702	1.656	in
16	B2U	391.1	0.0120	7.027	in	82	B2U	1243.2	6.5670	1.748	in
17	B3G	396.9	0.0	6.431	in	83	AG	1243.6	0.0	1.619	in
18	B1U	434.6	0.2223	4.860	in	84	B3G	1250.3	0.0	2.117	in
19	B1G	435.2	0.0	4.636	out	85	B2U	1256.9	3.9879	1.688	in
20	AG	447.9	0.0	4.705	in	86	AG	1307.9	0.0	2.804	in
21	B2G	468.4	0.0	3.662	out	87	B2U	1314.3	1.4489	5.351	in
22	B3U	471.4	0.0096	3.344	out	88	B3G	1330.9	0.0	2.622	in
23	B1U	478.7	4.0775	7.838	in	89	B2U	1334.3	6.7213	4.738	in
24	B2G	481.7	0.0	3.625	out	90	B1U	1341.6	0.0548	1.664	in
25	AU	498.4	0.0	4.021	out	91	AG	1343.7	0.0	2.616	in
26	B1U	528.0	7.8929	5.443	in	92	B3G	1380.5	0.0	3.956	in
27	B2U	538.8	1.0005	6.992	in	93	B2U	1385.5	1.7061	4.798	in
28	AG	544.8	0.0	7.369	in	94	AG	1391.1	0.0	5.888	in
29	B3G	554.1	0.0	6.283	in	95	B1U	1402.9	21.7449	4.820	in
30	B3G	570.5	0.0	7.373	in	96	AG	1403.2	0.0	4.662	in
31	B1G	571.4	0.0	3.697	out	97	B1U	1414.4	70.6773	3.040	in
32	B3U	579.7	4.0859	4.862	out	98	B1U	1432.5	3.5711	2.975	in
33	AG	590.1	0.0	6.498	in	99	AG	1454.3	0.0	4.361	in
34	B2G	628.2	0.0	4.653	out	100	AG	1480.8	0.0	2.185	in
35	B2U	637.1	0.4376	8.257	in	101	B1U	1491.1	9.3743	2.874	in
36	AU	637.5	0.0	4.044	out	102	B3G	1494.1	0.0	2.564	in
37	B1G	643.8	0.0	2.397	out	103	B3G	1507.6	0.0	3.579	in

38	AU	680.8	0.0	2.569	out	104	B2U	1508.9	0.9185	2.549	in
39	B1U	684.0	0.1339	6.041	in	105	B2U	1551.2	13.6049	4.224	in
40	B3U	703.8	3.1865	4.240	out	106	B3G	1556.0	0.0	3.646	in
41	B3G	738.3	0.0	6.509	in	107	B2U	1581.2	0.1469	4.748	in
42	B3U	765.7	35.1498	1.840	out	108	AG	1605.2	0.0	5.205	in
43	B2G	772.2	0.0	1.825	out	109	B1U	1622.1	5.2468	4.259	in
44	B1G	774.2	0.0	1.299	out	110	B1U	1631.4	35.5680	5.928	in
45	AU	778.9	0.0	1.481	out	111	B3G	1637.7	0.0	5.036	in
46	B2G	780.1	0.0	6.528	out	112	AG	1643.3	0.0	5.019	in
47	B1U	801.0	29.3050	5.549	in	113	B1U	1643.5	23.7887	5.019	in
48	AG	806.8	0.0	5.337	in	114	AG	1646.5	0.0	7.043	in
49	B1U	814.6	3.7775	5.626	in	115	B2U	1665.2	10.3815	6.047	in
50	B3U	829.6	144.9097	1.461	out	116	B3G	1668.4	0.0	7.071	in
51	B1G	832.4	0.0	1.695	out	117	B3G	3180.1	0.0	1.086	in
52	AG	838.7	0.0	7.249	in	118	B2U	3180.2	6.8479	1.086	in
53	B2G	843.8	0.0	3.257	out	119	B1U	3182.3	2.8223	1.086	in
54	B3U	844.2	1.3945	3.252	out	120	AG	3182.4	0.0	1.086	in
55	B2U	844.3	2.2445	6.140	in	121	B3G	3196.9	0.0	1.093	in
56	AU	884.4	0.0	1.490	out	122	B2U	3197.4	25.2615	1.094	in
57	B1G	889.1	0.0	1.379	out	123	B1U	3198.4	176.8030	1.093	in
58	B2G	904.2	0.0	1.546	out	124	AG	3199.2	0.0	1.094	in
59	B3U	909.3	0.4681	1.467	out	125	B3G	3206.6	0.0	1.090	in
60	AU	933.5	0.0	1.335	out	126	B1U	3206.8	0.0847	1.090	in
61	B2G	941.9	0.0	1.374	out	127	B2U	3216.3	10.1628	1.094	in
62	B1U	942.4	17.8005	4.901	in	128	AG	3216.5	0.0	1.094	in
63	B3G	965.8	0.0	6.425	in	129	B3G	3225.4	0.0	1.089	in
64	B1G	970.0	0.0	1.281	out	130	B1U	3225.4	10.5054	1.089	in
65	AU	971.0	0.0	1.279	out	131	B2U	3232.1	69.7886	1.090	in
66	B3U	979.0	1.5802	1.307	out	132	AG	3232.4	0.0	1.090	in



					
43	44	45	46	47	48
					
49	50	51	52	53	54
					
55	56	57	58	59	60
					
61	62	63	64	65	66
					
67	68	69	70	71	72
					
73	74	75	76	77	78

					
79	80	81	82	83	84
					
85	86	87	88	89	90
					
91	92	93	94	95	96
					
97	98	99	100	101	102
					
103	104	105	106	107	108
					
109	110	111	112	113	114

					
115	116	117	118	119	120
					
121	122	123	124	125	126
					
127	128	129	130	131	132